

This is a self-archived version of an original article. This version may differ from the original in pagination and typographic details.

Author(s): Trzaska, Wladyslaw; Heikkinen, Pauli; Danilov, A. N.; Demyanova, A. S.; Khlebnikov, S. V.; Malamut, T. Yu.; Maslov, V.; Ogloblin, A. A.; Sobolev, Yu. G.

Title: High-resolution scattering experiments at the K130 cyclotron in Jyväskylä

Year: 2018

Version: Accepted version (Final draft)

Copyright: © 2018 Elsevier B.V. All rights reserved.

Rights: CC BY-NC-ND 4.0

Rights url: <https://creativecommons.org/licenses/by-nc-nd/4.0/>

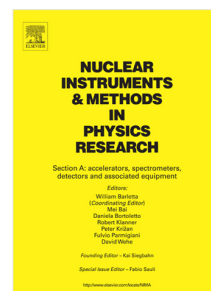
Please cite the original version:

Trzaska, W., Heikkinen, P., Danilov, A. N., Demyanova, A. S., Khlebnikov, S. V., Malamut, T. Y., Maslov, V., Ogloblin, A.A., & Sobolev, Y. G. (2018). High-resolution scattering experiments at the K130 cyclotron in Jyväskylä. *Nuclear Instruments and Methods in Physics Research Section A: Accelerators, Spectrometers, Detectors and Associated Equipment*, 903, 241-245.
<https://doi.org/10.1016/j.nima.2018.07.002>

Accepted Manuscript

High-resolution scattering experiments at the K130 cyclotron in Jyväskylä

W.H. Trzaska, P. Heikkinen, A.N. Danilov, A.S. Demyanova, S.V. Khlebnikov,
T.Yu. Malamut, V. Maslov, A.A. Ogloblin, Yu.G. Sobolev



PII: S0168-9002(18)30824-6
DOI: <https://doi.org/10.1016/j.nima.2018.07.002>
Reference: NIMA 60947

To appear in: *Nuclear Inst. and Methods in Physics Research, A*

Received date: 19 April 2018
Revised date: 8 June 2018
Accepted date: 2 July 2018

Please cite this article as: W.H. Trzaska, P. Heikkinen, A.N. Danilov, A.S. Demyanova, S.V. Khlebnikov, T.Y. Malamut, V. Maslov, A.A. Ogloblin, Y.G. Sobolev, High-resolution scattering experiments at the K130 cyclotron in Jyväskylä, *Nuclear Inst. and Methods in Physics Research, A* (2018), <https://doi.org/10.1016/j.nima.2018.07.002>

This is a PDF file of an unedited manuscript that has been accepted for publication. As a service to our customers we are providing this early version of the manuscript. The manuscript will undergo copyediting, typesetting, and review of the resulting proof before it is published in its final form. Please note that during the production process errors may be discovered which could affect the content, and all legal disclaimers that apply to the journal pertain.

1 Title:

2 **High-resolution scattering experiments**

3 **at the K130 cyclotron in Jyväskylä**

4 Author names and affiliations:

5 W. H. Trzaska^{a*}, P. Heikkinen^a, A. N. Danilov^b, A.S. Demyanova^b, S.V. Khlebnikov^c,

6 T. Yu. Malamut^b, V. Maslov^d, A. A. Ogloblin^b, Yu. G. Sobolev^d

7

8 *a - Department of Physics, University of Jyväskylä, FIN-40014 Jyväskylä, P.O. Box 35, Finland*

9 *b – NRC Kurchatov Institute, 1, Akademika Kurchatova pl., Moscow, 123182, Russia*

10 *c – V. G. Khlopin Radium Institute, 194021, St. Petersburg, Russia*

11 *d – Flerov Laboratory for Nuclear Research, JINR, 141980, Dubna, Moscow region, Russia*

12 *Corresponding author: wladyslaw.h.trzaska@jyu.fi

13

14 **Abstract**

15 An experimental setup for nuclear reaction studies induced by light and heavy ions is described.

16 It consists of a versatile Large Scattering Chamber equipped with two rotating tables for

17 mounting detectors. A dedicated beam diagnostic system is used to monitor the energy spectrum

18 of the beam on target. The system provides the necessary feedback for tuning of the K-130

19 cyclotron to reduce the energy spread of the accelerated beam by at least a factor of 3 down to

20 about 0.3% of the nominal energy while maintaining beam currents around 20 pA. At lower

21 beam currents a 0.1% energy spread can be achieved. This improvement makes a significant

22 impact on the scope of reaction studies possible to investigate at the Accelerator Laboratory of

23 the University of Jyväskylä. Similar solutions could be adapted by other cyclotron facilities.

24

25 Keywords: scattering experiments, cyclotron, beam optics, scattering chamber

26

1 **1 Introduction**

2 Cyclotrons are excellent tools for acceleration of charged ions. The K130 cyclotron at the
3 Accelerator Laboratory of the Physics Department at the University of Jyväskylä is a good
4 example of such a device. It was constructed primarily to satisfy the research needs of the two
5 main scientific users: the IGISOL (Ion Guide Separator On Line) [1,2] and the spectroscopy
6 group [3]. Of the primary concern were the stability of operation, large currents, wide range of
7 energies, and a broad selection of ion species. However, no provisions were made for the
8 reduction of the energy resolution of the beam. This became a serious drawback for the
9 extension of the nuclear reaction studies towards more demanding elastic scattering experiments.
10 The primary aim of these experiments is to obtain information on nucleus-nucleus potential from
11 nuclear rainbow scattering data [4,5]. One of the requirements of such studies is to have the
12 energy resolution of the detector and the energy spread of the beam smaller than the separation
13 between the relevant neighbouring excited states that are being investigated. In our case, a large
14 energy spread of the delivered cyclotron beams was the main problem. Consequently, to
15 continue the program of measuring the radii of nuclear excited states [6], a suitable solution had
16 to be found.

17 Problems with inadequate energy resolution of cyclotron beams are well known. Several
18 solutions have been proposed in the past that can be grouped into two categories: (i)
19 modifications of the cyclotron and its extraction system, and (ii) improvements of the extracted
20 beam using external, custom designed optical elements. A good example of the former is the 500
21 MeV H- cyclotron at TRIUMF. Already during the design and construction phases care was
22 taken to address the beam resolution issues. See for instance a dedicated TRIUMF report (TRI-
23 69-6) [7] discussing the ways to improve the spread of the raw 500 MeV beam from +600 keV –
24 520 keV down to ± 25 keV. However, designing a cyclotron for a well-defined purpose works
25 only if no alternative demands are made. Most of the time this is not the case. One of the reasons
26 why the Jyväskylä cyclotron is in such a high demand, delivering over 6000 hours of beam on

1 target per year, is the fact that it is a truly universal device, accelerating practically all elements
2 from hydrogen to lead and with energies from 2 MeV/u up to the bending limit of the main
3 magnet.

4 A good example of the second approach is a recent development at Liege [8] to improve
5 the energy resolution of the beam from a commercial AVF (Azimuthal Varying Field) cyclotron
6 constructed by the French CGR-MeV company to make it useable for RBS (Rutherford Back
7 Scattering) analysis. There the cyclotron beam is deflected by a switching magnet into a pair of
8 90-degree left-right bending magnets forming an achromatic doublet. The energy selection is
9 accomplished by 3 collimators, each 1.7 mm diameter, at the entrance, middle and at the exit of
10 the doublet. This arrangement allows to reduce energy resolution of a 14 MeV alpha beam from
11 over 50 keV to about ± 2 keV. The improvement by over an order of magnitude is commendable
12 but the down side of this approach is the cost and space needed to accommodate 3 additional
13 magnets and the relevant beam pipe elements. Such a solution would not be currently possible in
14 Jyväskylä.

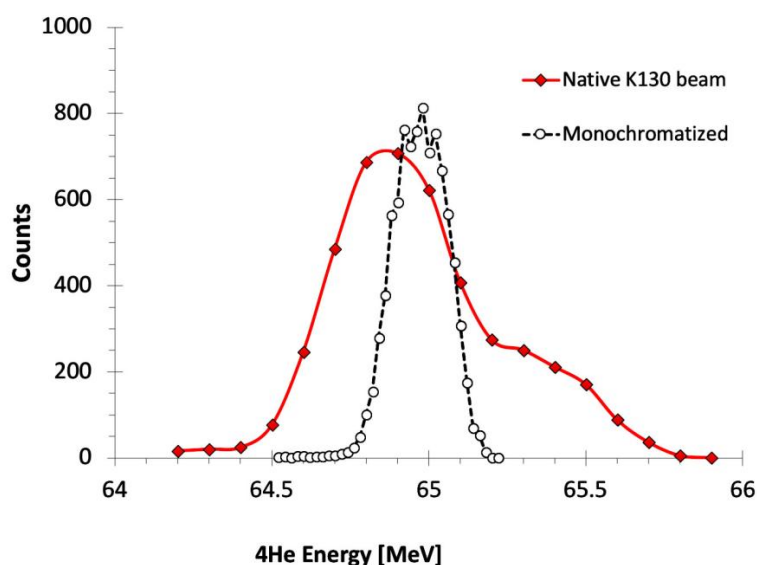
15 What we are describing here is a third approach: to improve the energy resolution relying
16 exclusively on standard beam optics elements, without the need to modify the cyclotron
17 construction nor build dedicated beam lines. Obviously, the obtained results in such a simple
18 manner cannot be compared with the top achievements produced by a specially designed setup.
19 Nevertheless, whenever there is no time, no funding, and/or no space to build a proper high-
20 resolution beam line, our solution provides a viable substitute.

21

22 **2 Beam monochromatization at K130 cyclotron**

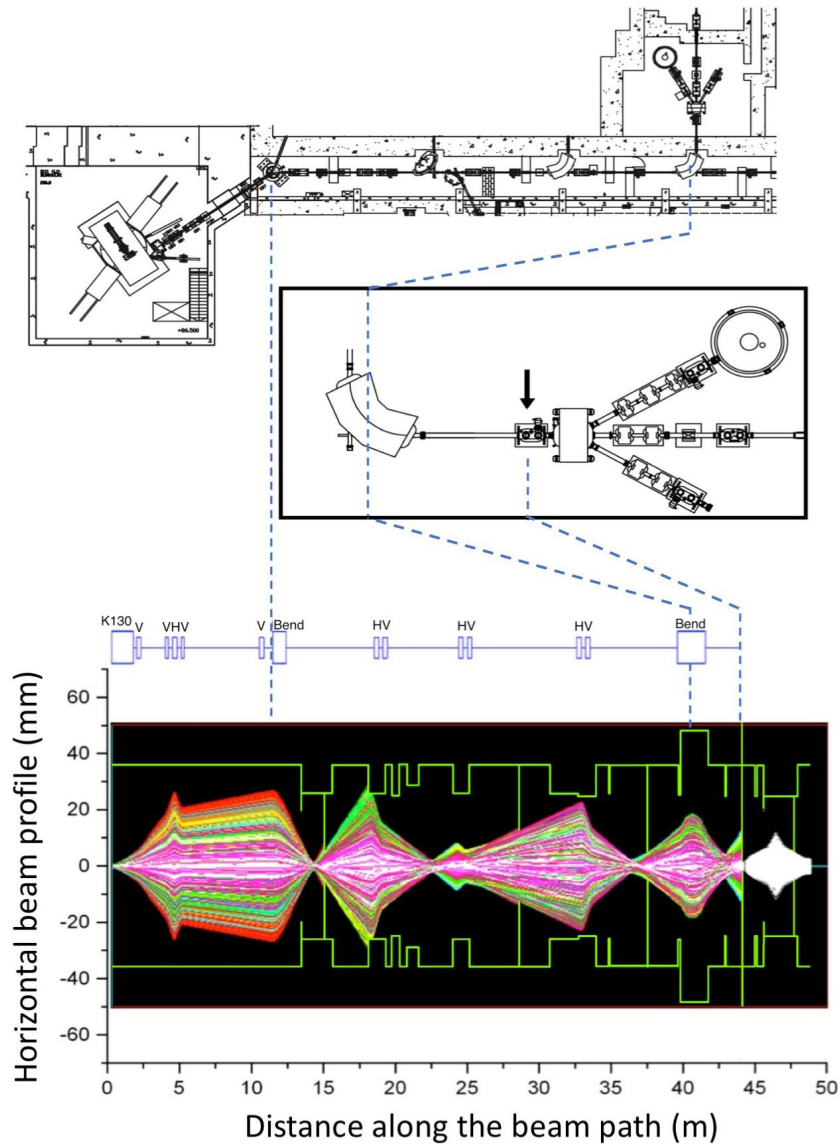
23 The energy spread of an ion beam from a cyclotron results mainly from the fact that the extracted
24 beam bunch contains ions not just from one but also from the two or three final turns of the
25 acceleration spiral. One may even estimate the magnitude of the expected spread by dividing the
26 final energy by the number of turns in the cyclotron and multiplying it by two or three to account

1 for the 2-3 orbit extraction. There is also some dependence on the phase acceptance of the
 2 cyclotron. In the Jyväskylä K130 cyclotron the number of turns is about 720, 290 and 190 for the
 3 first, second and third harmonic modes, respectively, and the phase acceptance is 30 – 40
 4 degrees (in RF-phase). For example, a 65 MeV alpha beam accelerated with the second
 5 harmonic mode would have a natural energy spread of 0.5 – 1 %.



6
 7 *Fig.1. An example of a dramatic improvement of the beam profile (black circles connected by a*
 8 *dashed line) using monochromatization method described in this paper. The native cyclotron*
 9 *beam (red squares connected by a solid line) has a broad, asymmetric, two-humped structure.*

11 Clearly, the 0.5 – 1% spread of the direct cyclotron beam is not always acceptable. In
 12 addition, depending on the proportion of ions extracted from different orbits, there is a double or
 13 even triple structure visible in the energy spectrum of the beam delivered to the target. Energy
 14 spectra plotted in Fig. 1 give a clear illustration of both the problem and the proposed solution.
 15 The two curves show the beam profile before and after the monochromatization procedure
 16 described below. This example is for a typical 65 MeV ^4He beam scattered in the forward
 17 direction (below the grazing angle) from a thin gold target and registered by a silicon detector.



1

2 *Fig.2. Simulated horizontal beam profile along the path from the cyclotron extraction point to*
 3 *the target. The colour of a trajectory represents the energy of the ion. The energy defining slit*
 4 *located at around 44 m pass only particles with the desired energy (white trajectories). The*
 5 *green outline indicates the internal radius of the beam pipe. The vertical green lines represent*
 6 *collimators. The active elements of the beam line are shown in-scale above the main plot while*
 7 *the actual layout of the beam line is shown on the top. The inset shows the location of the*
 8 *diagnostic box with the energy defining slit.*

9

1 Since the K130 cyclotron does not have phase slits for decreasing the phase acceptance
2 and since it is extremely difficult to obtain a single turn extraction, we have chosen to minimize
3 the beam energy spread by using a narrow slit further down along the beam line at the point
4 where the dispersion (D) of the beam is large. The dispersion starts to develop already at the
5 fringe field of the cyclotron, right after the extractor. The dispersion is controlled with
6 quadrupole magnets in the same manner as the beam and it has source terms in each bending
7 magnet (dipole).

8 Fig. 2 shows the result of ion optics simulation of the beam evolution after extraction
9 from the cyclotron. The active elements are shown, above the trajectory plots, as rectangles:
10 K130 is the cyclotron magnet, V and H indicate vertically and horizontally focusing
11 quadrupoles, BEND are the bending dipoles. The X-axis shows the distance in meters from the
12 accelerator towards the target in the centre of LSC (at about 48.9 m). The vertical lines represent
13 the slits. The Y-axis shows the horizontal beam size in millimetres. The simulations were made
14 for a 21.5 MeV deuteron beam. The colour of the trajectory line indicates the energy. The
15 desired energy of 21.5 MeV is white. The more vibrant the colour of the trajectory line (or the
16 darker the line in B&W representation) the more it deviates from the desired value. The initial
17 energy spread was $\pm 0.4\%$. The cyclotron fringe field has been approximated by piecewise
18 constant dipole fields with different field gradients. The initial beam emittances have been
19 adjusted so that the calculation corresponds roughly to the measured beam dimensions in the
20 beam line.

21 The applied beam optics shown on Fig. 2 has been optimized to get the maximum
22 transmission from the cyclotron to the target. Normally, when no attention is paid to the energy
23 spread, the dispersion at the 3 mm narrow slit, located at the image point of the 90° double-
24 focusing dipole magnet, is approximately 4 m. However, in order to control the energy spread,
25 the optics was modified with an additional intermediate focus upstream in the beam line. It
26 increased the dispersion to 6 m at the 3 mm x 15 mm energy defining slit located at about 44 m

1 from the cyclotron and depicted as a vertical line on Fig.2. The effectiveness of this approach is
2 clearly visible on the plot as all vibrantly coloured trajectories are removed by the slit.

3 Ultimately, the energy spread of the beam through a 3 mm slit would be 0.1 % at a focal
4 point, where $D = 6$ m, if the width of a monochromatic beam was also 3 mm. By slightly
5 increasing the horizontal width of a monochromatic beam at this point the intensity of the
6 transmitted beam increased while the energy spread was increased to 0.3 % reaching the desired
7 compromise for the physics case discussed below.

8 The physical location of the slit is inside of the diagnostic box placed just before the
9 entrance to the 30-degree switching magnet directing the beam to the LSC. The actual layout of
10 the beam line is shown on the top part of Fig.2. The locations and the relevant setting of the
11 beam control elements are listed in Tab.1. The section between the 90° double-focusing dipole
12 magnet and the LSC is shown in more detail on the inset in Fig.2. A photo of the LSC is shown
13 in Fig. 3.

14 The downside of the improved energy resolution is the loss of beam intensity. Since
15 most of our measurements require beam currents of about 30 nA on the target, the practically
16 achievable beam resolution from the K130 cyclotron is about 0.2 - 0.3 %. However, at lower
17 beam intensities, we were able to reach down to 0.1% resolution, as predicted by simulations
18 depicted in Fig. 2.

19 The other point of concern is the background induced by the 3 mm energy-defining slit
20 where a substantial portion of the beam is stopped causing noticeable activation. The resulting
21 gamma-ray background is dealt with additional shielding. Nevertheless, since the slit is nearly 5
22 m upstream from the target and is separated by several optical elements including three
23 collimators removing the remnants of the beam halo, we do not observe inside of the LSC any
24 background due to beam scattering (Fig. 4). In addition, already inside the LSC, there is a
25 provision for the final collimators. They may be inserted into the tube, visible in Fig. 3 and 5,
26 protruding from the entrance into the LSC towards the target.

1



2

3 *Fig. 3. Photo of the LSC with the upper hemisphere lifted for installation of detectors and*
4 *targets. The beam enters the chamber from the right side, passes through the collimator tube*
5 *towards the target holder visible in the centre, and exits through the large circular opening at*
6 *the back of the chamber (on the left side on the photo) leading towards the Faraday Cup. The*
7 *detectors are mounted to the rails fixed to the lower and the upper rotating table. The shortage*
8 *of space around the chamber excludes the possibility to install external monochromators.*

9

10 **3 Large Scattering Chamber**

11 The Large Scattering Chamber (LSC) is the main tool in the study of nuclear reactions at the
12 K130 cyclotron. The nominal diameter of the LSC (Fig.3 and 5) is 1.5 meter. Inside of the
13 chamber there are two circular and independently rotatable mounting platforms: one on the
14 lower and one of the upper hemisphere of the LSC. The platforms provide support for mounting
15 and precise position adjustment of particle detectors. Each platform has a set of equally spaced
16 holes and rings to facilitate accurate and reproducible placement and adjustment of the detectors

1 and collimators. Detectors may be moved to any desired distance from the target within the
2 limits of the chamber. The positioning accuracy is ± 0.25 mm. At the central axis of the LSC
3 there is a steel rod supporting a ladder-shaped target holder capable of accommodating up to six
4 targets. The rod can rotate as well as move up and down to allow multiple targets to be placed on
5 the path of the beam without the need to break the vacuum. Remote control and read-out of the
6 position of the platforms and targets is possible.

7 The incoming beam, before reaching the target, has to pass through a collimator tube with
8 three slots for inserting diaphragms: Slot 1 is at the entrance to the chamber, Slot 2 is at the
9 distance of 36 cm from the target, and Slot 3 is at 30 cm from the target. A typical set of
10 diaphragms is 9-9-10 with the largest (10 mm diameter opening) in the Slot 3 – the one closes to
11 the target. The diaphragms are made of a 2 mm thick tantalum plate. The supporting stainless-
12 steel tube has the outside diameter of 30 mm.

13 At the place where the beam exits from the LSC there is a large opening leading to the
14 continuation of the beam pipe and ending with a Faraday Cup (FC). FC is surrounded by lead
15 bricks and concrete blocks to lower the radiation levels. The beam tuning is performed by
16 monitoring the current from the FC and from the diagnostic box upstream from the LCS. In
17 addition, we use optical feedback from a scintillation plate placed in the target position. The
18 plate has an opening corresponding to the desired diameter of the beam spot. This way the most
19 intense beam passes through while the fine-tuning of the beam position is done observing and
20 minimizing the scintillation of the beam halo. The beam spot is typically 3 mm in diameter.

21 The hemispherical top lid of the LSC, constructed from a thin sheet of stainless steel, has
22 been designed to minimize neutron and gamma-ray absorption. This provision has been made to
23 allow for measurements of particle-gamma correlations and for measurements of neutron
24 emission, for instance, in coincidence with particle induced fission events.

25 LSC is permanently attached to the beam line of the K130 cyclotron and is located in a
26 dedicated cavern (Fig. 3). The total length of the beam line is about 49 m from the cyclotron to

1 the centre of the LSC. The magnetic elements along the beam line include, in addition to several
2 quadrupole doublets and triplets, also a 90-degree and a 30-degree dipole (Fig. 4). There are
3 numerous diagnostic boxes along the path of the beam. The full list of the optical elements is
4 provided in Tab.1.

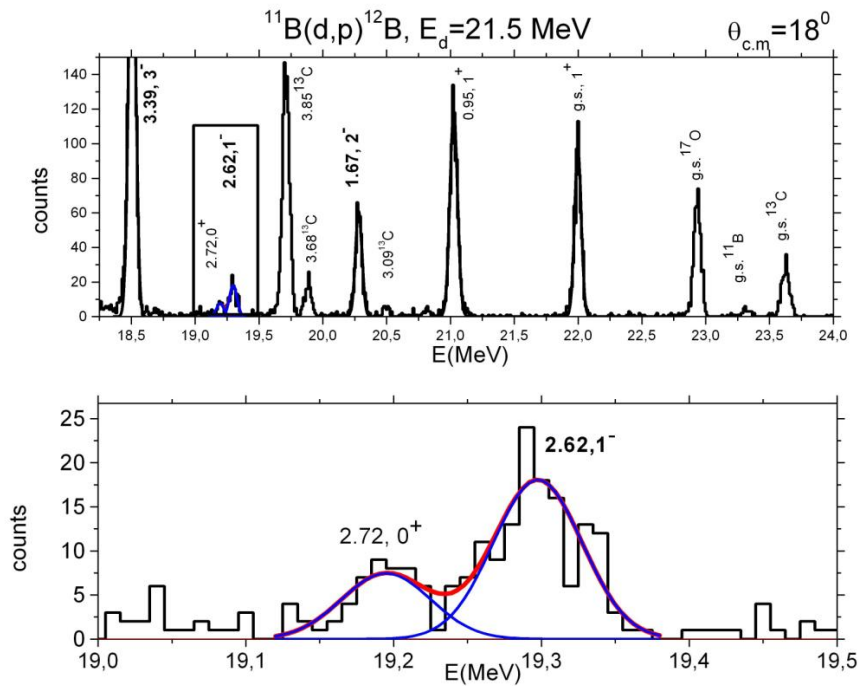
5

6 **4 Applications of monochromatized beam**

7 Currently the main application of the improved energy resolution of the K130 cyclotron is the
8 search for nuclear excited states with abnormal radii. Alfred Baz has predicted the existence of
9 such states already in 1959 [9] but until recently there were no means of direct verification. Only
10 non-direct methods were available like comparison of the form factors extracted from inelastic
11 electron scattering with those obtained from theoretical calculations assuming different radii
12 [10,11, and the references therein]. Our group has proposed an alternative approach [6]. Over the
13 past decade we have studied two types of nuclear structures with unusual properties: the excited
14 states of light nuclei possessing α -cluster structure, and neutron halos. Analysis of our data
15 provided new evidence for the existence of several excited states of ${}^9\text{Be}$, ${}^{11}\text{Be}$, ${}^{11}\text{B}$, ${}^{12}\text{C}$, ${}^{13}\text{C}$ [6]
16 with radii exceeding the radii of their ground states by $\sim 20\text{--}30\%$. These dilute states may be
17 considered as nuclear size isomers. The main conclusions are as follows: 1) halos are not
18 restricted to the drip-line nuclei; 2) halos are formed not only in the ground states of nuclei, but
19 in excited states as well (for instance, the first excited state of ${}^{13}\text{C}$); 3) halos exist not only in
20 particle-stable states, but also in continuum (halo in the excited states of ${}^9\text{Be}$ and ${}^{11}\text{Be}$).
21 Consequently, the study of halo in continuum became a new direction in our investigation of
22 exotic nuclei. Further, investigation of alpha-cluster states in ${}^{12}\text{C}$, ${}^{11}\text{B}$, ${}^{13}\text{C}$ gave us a new tool in
23 the search for hypothetical giant states. The most recent compilation of our investigations can be
24 found in [6].

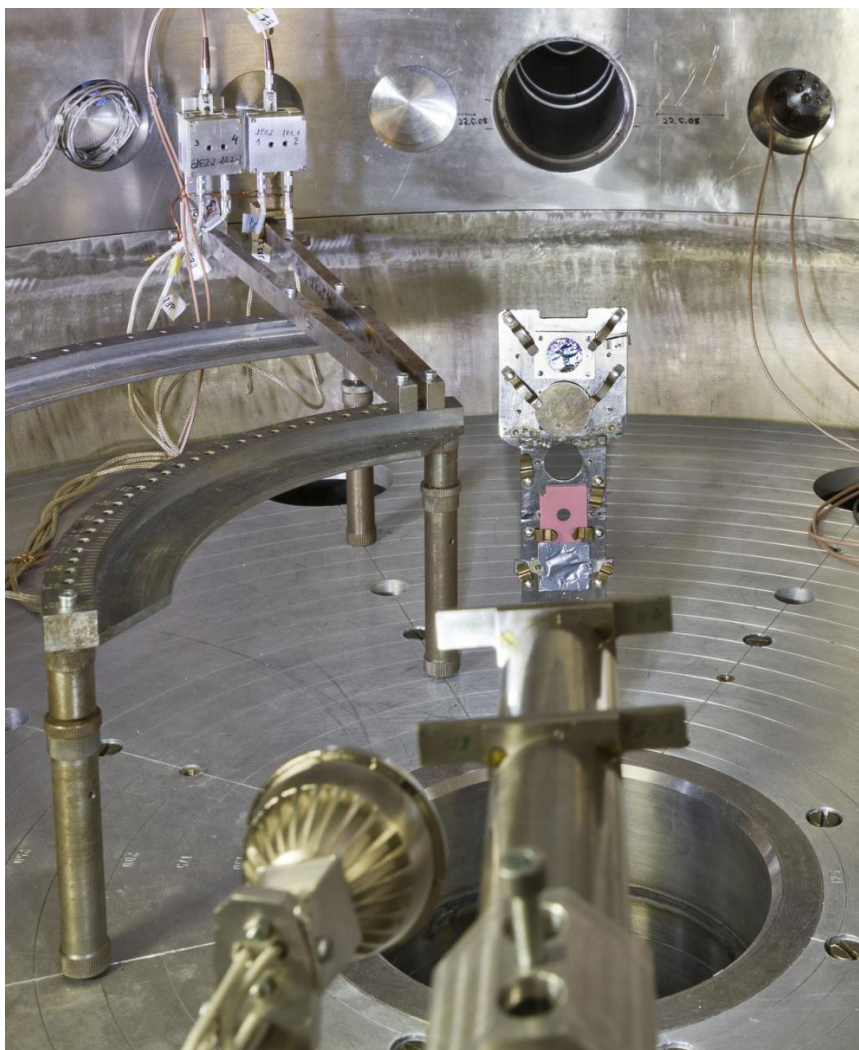
25 Among our latest experiments is the study of the ${}^{11}\text{B}(\text{d,p}){}^{12}\text{B}$ reaction (to be published)
26 aiming to identify a possible neutron halo doublet $1^- - 2^-$ in ${}^{12}\text{B}$. A sample spectrum is presented

1 in Fig.4. A typical detector configuration is shown on Fig. 5. To reach the required energy and
 2 angular resolution, the detectors were placed at the largest distance from the target (~60 cm) and
 3 were covered with diaphragms with the diameter corresponding to the diameter of the beam spot
 4 on the target (3 mm). The spectrum on Fig. 4 was chosen to illustrate the benefit of the improved
 5 beam resolution to reliably separate the 1^- , 2.62 MeV state from the neighbouring 2.72 MeV
 6 state in ^{12}B .



7
 8 Fig. 4. Top: Proton spectrum measured at 18° c.m. from the $^{11}\text{B}(d,p)^{12}\text{B}$ reaction. Bottom: a
 9 section of the spectrum showing the separation of the neighbouring levels in ^{12}B made possible
 10 by the monochromatization of the beam from the K130 cyclotron.

11



1
2 *Fig. 5. Photo of the interior of the LHC during a typical scattering experiment. The view is along*
3 *the path of the beam. The collimator tube in the foreground points towards the target holder and*
4 *the circular opening at the back of the chamber leading towards the Faraday Cup. The detectors*
5 *are attached to the rails fixed to the lower and upper rotating table. For clarity, only detectors*
6 *on the lower table are visible on the photo. To the left of the collimator tube is a light source*
7 *that, if needed, may be used also in vacuum.*

8

9 **5 Conclusions**

10 An experimental setup for nuclear reactions studies induced by light and heavy ions is
11 described. It consists of a versatile Large Scattering Chamber equipped with two rotating tables

1 to mount detectors. The LSC facility continues to be widely used in many experiments,
2 especially in the study of nuclear rainbow scattering [4,5], measurement of radii of the excited
3 short-lived states [6] and in energy loss measurements of heavy ions in various materials [12].

4 A dedicated beam diagnostic system is used for monitoring of the energy spread of the
5 beam on target. The system provides the necessary feedback for tuning of the K-130 cyclotron to
6 improve the energy spread of the accelerated beam by at least a factor of three down to about
7 0.3% of the nominal energy while maintaining beam currents around 20 pA. At lower beam
8 currents a 0.1% energy spread was achieved. This improvement makes a significant impact on
9 the scope of reaction studies possible to investigate at the Accelerator Laboratory of the
10 University of Jyväskylä. Similar solutions could be adapted by other cyclotron facilities without
11 the need of significant changes to the design of the accelerator and without the need to construct
12 external monochromators.

13

14 **Acknowledgements**

15 The work was supported in part by the mobility grants of the Finnish Academy of Sciences and
16 by the grant 18-12-00312 of the Russian Science Foundation.

17

18 **References**

- 19 [1] *Hyperfine Interactions* Vol. 223, Issues 1-3, 2014.
20 [2] *The European Physical Journal A* Vol. 48, Issue 4, 2012.
21 [3] R. Julin, T. Grahn, J. Pakarinen, & P. Rahkila, *Journal of Physics G: Nuclear and Particle*
22 *Physics*, 43 (2). [doi:10.1088/0954-3899/43/2/024004](https://doi.org/10.1088/0954-3899/43/2/024004).
23 [4] A.A.Ogloblin, S.A.Goncharov, Yu.A.Glukhov, A.S.Demyanova, M.V.Rozhkov,
24 V.P.Rudakov and W.H.Trzaska, *Physics of Atomic Nuclei*, Vol.66 No.8 2003, pp. 1478-1488.
25 [5] S. Ohkubo, Y. Hirabayashi, A. A. Ogloblin, Yu. A. Gloukhov, A. S. Dem'yanova, and W.
26 H. Trzaska, *Phys. Rev. C* **90**, 064617 (2014).

- 1 [6] A. A. Ogloblin, A. N. Danilov, A. S. Demyanova, S. A. Goncharov, T. L. Belyaeva, and
 2 W. Trzaska “NUCLEAR SIZE ISOMERS: THE EXCITED STATES OF LIGHT NUCLEI
 3 WITH CLUSTER STRUCTURE AND NONSTANDARD SIZES”, “Nuclear Particle
 4 Correlations and Cluster Physics” book edited by Schröder Wolf-Udo (University of
 5 Rochester, USA), 311-338 (2017).
- 6 [7] J.R.Richardson, Energy Resolution in a 500 MeV H- Cyclotron, TRI-69-6, TRIUMF June
 7 1969.
- 8 [8] G. Chêne, S. Bols, T. Dupuis, A. Marchal, F. Mathis, H.-P. Garnir, D. Strivay, Nuclear
 9 Instruments and Methods in Physics Research B **273**, 208 (2012).
- 10 [9] A. I. Baz, Threshold effects in nuclear reactions, Advances in Physics 8 (32), 349–374
 11 (1959); Resonance effects in the scattering of particles near a reaction threshold, JETP 36,
 12 1762–1766 (1959).
- 13 [10] M. Chernykh, H. Feldmeier, T. Neff, P. von Neumann-Cosel, and A. Richter, Phys. Rev.
 14 Lett. 98, 032401 (2007), DOI: 10.1103/PhysRevLett.98.032501.
- 15 [11] M. Kamimura, Nucl. Phys. A351,456(1981).
- 16 [12] W.H.Trzaska, et al. Nucl. Instr. and Methods B 418 (2018) 1.
 17 [doi:10.1016/j.nimb.2017.12.025](https://doi.org/10.1016/j.nimb.2017.12.025)

18
 19 Table 1. List of beam optic elements between the K130 cyclotron and the LSC. The elements
 20 are also shown in Fig.3. The distance is measured to the center of each element. Horizontally
 21 and vertically focusing quadrupoles are denoted as QUAD(H) and QUAD(V). If a collimator
 22 has a choice of setting, all are listed, and the chosen value is marked in bold. The bending
 23 angle of a dipole (in degrees) is shown in brackets.

Distance (m)	Optic Element	Setting
1.860	QUAD(V)	
3.800	QUAD(V)	
4.350	QUAD(H)	
4.900	QUAD(V)	

10.347	QUAD(V)	
11.562	Dipole(35)	
13.249	Collimator	$\Phi = 5, 10, 15$ mm
18.235	QUAD(H)	
18.835	QUAD(V)	
24.135	QUAD(H)	
24.735	QUAD(V)	
32.938	QUAD(H)	
33.538	QUAD(V)	
37.447	Collimator	$\Phi = 5, 10, 15$ mm
40.714	Dipole(90)	
44.054	Slit	3 mm
44.671	Dipole(30)	
45.586	Collimator	$\Phi = 5, 10, 15$ mm
45.815	QUAD(V)	
46.415	QUAD(H)	
47.015	QUAD(V)	
47.708	Collimator	$\Phi = 10$ mm
48.915	Target	

1